Supplementary Material

Supplementary Tables

Number of participants with and without ICD and/or depression

*Supplementary Table 1 - **Number of participants with and without ICD and/or depression***

	HC	ON	OFF	PD	ALL
NUMBER OF PARTICIPANTS	60 (100%)	138 (100%)	61 (100%)	199 (100%)	259 (100%)
ICD	/	36 (26%)	12 (20%)	48 (24%)	96 (37%)
ICD WITHOUT DEP	/	22 (16%)	8 (13%)	30 (15%)	78 (30%)
DEP	0 (0%)	34 (25%)	10 (16%)	44 (22%)	44 (17%)
DEP WITHOUT ICD	0 (0%)	20 (14%)	6 (10%)	26 (13%)	26 (10%)
WITHOUT ICD OR DEP	/	82 (59%)	43 (70%)	125 (63%)	137 (53%)
WITH ICD AND DEP	/	14 (10%)	4 (7%)	18 (9%)	18 (7%)

Mean accuracy per valence, for each ICD group

*Supplementary Table 2 - **Mean accuracy and standard deviation per valence, for each ICD group***

	GAIN	LOSS
ALL PD ON	0.65 (0.23)	0.63 (0.17)
ALL PD OFF	0.67 (0.23)	0.6 (0.16)
ALL HC	0.7 (0.22)	0.66 (0.13)
ICD PD ON	0.67 (0.2)	0.59 (0.18)
ICD PD OFF	0.53 (0.26)	0.61 (0.2)
ICD HC	0.71 (0.23)	0.66 (0.13)
NO ICD PD ON	0.64 (0.24)	0.64 (0.17)
NO ICD PD OFF	0.7 (0.21)	0.61 (0.15)
NO ICD HC	0.65 (0.18)	0.67 (0.13)

Model Space

Supplementary table 3 & 4 present respectively the model space & model parameters used in the current paper. We used a principled approach to set up the model space. For each behavioral parameter (i.e. accuracy, wsls-behavior & reaction time) we began by assessing the MEDICATION x VALENCE effect. Second, we assessed the interaction with ICD and depression. To do so, we added the interaction with the binary ICD or depression regressor (based on clinical cut-off values for the QUIP-rs & BDI). In further, supplementary analyses, we assessed whether any effect of a binary regressor was accompanied also by a continuous effect, by using the continuous QUIP-rs & BDI scores directly. Third, we assessed whether the effect of interest (i.e. MEDICATION x VALENENCE x CLASS-ICD) survived correction for possible confounding regressors, such as psychomotor speed (symbols & digits modality test). Valence, and for WSLS-analysis outcome on the previous trial, were added as random slopes.

*Supplementary Table 3 - **Model Space** – We investigated reaction time, accuracy and WSLS behavior based on BRMS mixed effect models presented in this table. For an explanation of model parameters, see supplementary table 4; model parameters.*

Dependent Variable	Confounding factor	Model	Effect of interest	Lower bound 95% CI	Upper bound 95% CI	Significant
Reaction Time	N.A.	response_time ~ valence * group + (1 + valence | SubjectNumber)	valence * group	-0.014	0.011	FALSE
Reaction Time	N.A.	response_time ~ valence * group * class_quiprs + (1 + valence | SubjectNumber)	valence * group * class_quiprs	-0.033	-0.002	TRUE
Reaction Time	N.A.	response_time ~ valence * group * z_QUIPRS_TOT + (1 + valence | SubjectNumber)	valence * group * z_QUIPRS_TOT	-0.024	0.006	FALSE
Reaction Time	N.A.	response_time ~ valence * group * class_bdi_simplified + (1 + valence | SubjectNumber)	valence * group * class_bdi_simplified	-0.014	0.020	FALSE
Reaction Time	N.A.	response_time ~ valence * group * z_BDI + (1 + valence | SubjectNumber)	valence * group * z_BDI	-0.015	0.013	FALSE
Reaction Time	Depression Diagnosis	response_time ~ valence * group * class_quiprs + class_bdi_simplified + (1 + valence | SubjectNumber)	valence * group * class_quiprs	-0.033	-0.002	TRUE
Reaction Time	Depression Score	response_time ~ valence * group * class_quiprs + z_BDI + (1 + valence | SubjectNumber)	valence * group * class_quiprs	-0.033	-0.002	TRUE
Reaction Time	Anxiety Score	response_time ~ valence * group * class_quiprs + z_STAI + (1 + valence | SubjectNumber)	valence * group * class_quiprs	-0.034	-0.002	TRUE
Reaction Time	LEDD	response_time ~ valence * group * class_quiprs + z_LEDD + (1 + valence | SubjectNumber)	valence * group * class_quiprs	-0.034	-0.002	TRUE
Reaction Time	Dopamine Agonist Use	response_time ~ valence * group * class_quiprs + useAgo + (1 + valence | SubjectNumber)	valence * group * class_quiprs	-0.031	0.001	FALSE
Reaction Time	Symbol & Digit task score	response_time ~ valence * group * class_quiprs + SymbolDigit + (1 + valence | SubjectNumber)	valence * group * class_quiprs	-0.033	-0.002	TRUE
Reaction Time	Months Since Diagnosis	response_time ~ valence * group * class_quiprs + MonthsSinceDiag + (1 + valence | SubjectNumber)	valence * group * class_quiprs	-0.033	-0.002	TRUE
Win-Stay-Lose-Shift	N.A.	StayShift_num ~ valence * group * OutcomeM1 + (1 + valence * OutcomeM1 | SubjectNumber)	valence * group * OutcomeM1	-0.032	0.072	FALSE
Win-Stay-Lose-Shift	N.A.	StayShift_num ~ valence * group * OutcomeM1 * class_quiprs + (1 + valence * OutcomeM1 | SubjectNumber)	valence * group * OutcomeM1 * class_quiprs	0.026	0.151	TRUE
Win-Stay-Lose-Shift	N.A.	StayShift_num ~ valence * group * OutcomeM1 * z_QUIPRS_TOT + (1 + valence * OutcomeM1 | SubjectNumber)	valence * group * OutcomeM1 * z_QUIPRS_TOT	-0.004	0.117	FALSE
Win-Stay-Lose-Shift	N.A.	StayShift_num ~ valence * group * OutcomeM1 * class_bdi_simplified + (1 + valence * OutcomeM1 | SubjectNumber)	valence * group * OutcomeM1 * class_bdi_simplified	-0.110	0.023	FALSE
Win-Stay-Lose-Shift	N.A.	StayShift_num ~ valence * group * OutcomeM1 * z_BDI + (1 + valence * OutcomeM1 | SubjectNumber)	valence * group * OutcomeM1 * z_BDI	-0.005	0.107	FALSE
Win-Stay-Lose-Shift	Depression Diagnosis	StayShift_num ~ valence * group * OutcomeM1 * class_quiprs + class_bdi_simplified + (1 + valence * OutcomeM1 | SubjectNumber)	valence * group * OutcomeM1 * class_quiprs	0.024	0.150	TRUE
Win-Stay-Lose-Shift	Depression Score	StayShift_num ~ valence * group * OutcomeM1 * class_quiprs + z_BDI + (1 + valence * OutcomeM1 | SubjectNumber)	valence * group * OutcomeM1 * class_quiprs	0.026	0.151	TRUE
Win-Stay-Lose-Shift	Anxiety Score	StayShift_num ~ valence * group * OutcomeM1 * class_quiprs + z_STAI + (1 + valence * OutcomeM1 | SubjectNumber)	valence * group * OutcomeM1 * class_quiprs	0.026	0.150	TRUE
Win-Stay-Lose-Shift	LEDD	StayShift_num ~ valence * group * OutcomeM1 * class_quiprs + z_LEDD + (1 + valence * OutcomeM1 | SubjectNumber)	valence * group * OutcomeM1 * class_quiprs	0.024	0.150	TRUE
Win-Stay-Lose-Shift	Dopamine Agonist Use	StayShift_num ~ valence * group * OutcomeM1 * class_quiprs + useAgo + (1 + valence * OutcomeM1 | SubjectNumber)	valence * group * OutcomeM1 * class_quiprs	0.018	0.148	TRUE
Win-Stay-Lose-Shift	Symbol & Digit task score	StayShift_num ~ valence * group * OutcomeM1 * class_quiprs + SymbolDigit + (1 + valence * OutcomeM1 | SubjectNumber)	valence * group * OutcomeM1 * class_quiprs	0.025	0.151	TRUE
Win-Stay-Lose-Shift	Months Since Diagnosis	StayShift_num ~ valence * group * OutcomeM1 * class_quiprs + MonthsSinceDiag + (1 + valence * OutcomeM1 | SubjectNumber)	valence * group * OutcomeM1 * class_quiprs	0.028	0.155	TRUE
Accuracy	N.A.	correct_response_num ~ valence * group + (1 + valence | SubjectNumber)	valence * group	-0.171	0.049	FALSE
Accuracy	N.A.	correct_response_num ~ valence * group * class_quiprs + (1 + valence | SubjectNumber)	valence * group * class_quiprs	0.028	0.297	TRUE
Accuracy	N.A.	correct_response_num ~ valence * group * z_QUIPRS_TOT + (1 + valence | SubjectNumber)	valence * group * z_QUIPRS_TOT	0.008	0.269	TRUE
Accuracy	N.A.	correct_response_num ~ valence * group * class_bdi_simplified + (1 + valence | SubjectNumber)	valence * group * class_bdi_simplified	-0.242	0.051	FALSE
Accuracy	N.A.	correct_response_num ~ valence * group * z_BDI + (1 + valence | SubjectNumber)	valence * group * z_BDI	-0.023	0.224	FALSE
Accuracy	Depression Diagnosis	correct_response_num ~ valence * group * class_quiprs + class_bdi_simplified + (1 + valence | SubjectNumber)	valence * group * class_quiprs	0.028	0.300	TRUE
Accuracy	Depression Score	correct_response_num ~ valence * group * class_quiprs + z_BDI + (1 + valence | SubjectNumber)	valence * group * class_quiprs	0.028	0.297	TRUE
Accuracy	Anxiety Score	correct_response_num ~ valence * group * class_quiprs + z_STAI + (1 + valence | SubjectNumber)	valence * group * class_quiprs	0.027	0.298	TRUE
Accuracy	LEDD	correct_response_num ~ valence * group * class_quiprs + z_LEDD + (1 + valence | SubjectNumber)	valence * group * class_quiprs	0.023	0.294	TRUE
Accuracy	Dopamine Agonist Use	correct_response_num ~ valence * group * class_quiprs + useAgo + (1 + valence | SubjectNumber)	valence * group * class_quiprs	0.015	0.281	TRUE
Accuracy	Symbol & Digit task score	correct_response_num ~ valence * group * class_quiprs + SymbolDigit + (1 + valence | SubjectNumber)	valence * group * class_quiprs	0.025	0.295	TRUE
Accuracy	Months Since Diagnosis	correct_response_num ~ valence * group * class_quiprs + MonthsSinceDiag + (1 + valence | SubjectNumber)	valence * group * class_quiprs	0.015	0.290	TRUE

Model parameters

*Supplementary Table 4 – **Model parameters** – An overview of all model parameters used for analysis. Parameter starting with a Z are z-scored.*

REGRESSOR NAME	REGRESSOR TYPE	REGRESSOR DESCRIPTION	REGRESSOR OPTIONS
VALENCE	Binary	Trial type of the current variable	GAIN (1) or LOSS (0)
GROUP (I.E. MEDICATION)	Binary	Group to which the subject belonged. For each option, a separate model was run.	ON (1) vs OFF (0) ON (1) vs HC (0) OFF (1) vs HC) (0)
OUTCOMEM1	Binary	Indicating whether the previous trial was either rewarded (+€10 for GAIN trials or €0 for LOSS trials) or punished (€0 for GAIN trials or €-10 for LOSS trials).	Rewarded (1) or punished (0)
Z_BDI	Continuous	Summary score of the BDI questionnaire, indicating the degree of depression	
Z_QUIPRS_TOT	Continuous	Summary score of the QUIP-rs questionnaire, indicating the degree of impulsivity	
Z_STAI	Continuous	Summary score of the STAI questionnaire, indicating the degree of anxiety in the current state (opposed to trait)	
CLASS_QUIPRS	Binary	Classification of clinical ICD based on (CITE)	ICD (1) and non-ICD (0)
CLASS_BDI_SIMPLIFIED	Binary	Classification of clinical depression	Depressed (1) and non-depressed (0)
CORRECT_RESPONSE_NUM	Binary	Shows whether the correct cue was chosen on a given trial	Correct (1) or incorrect (0)
STAYSHIFT_NUM	Binary	Shows whether the same cue as the previous trial of that trial type was chosen for a given trial	Same (1) or other (0)
RESPONSE_TIME	Continuous	Reaction time between cue presentation and response in milliseconds	
Z_LEDD	Continuous	Levodopa Equivalent Daily Dose	
USEAGO	Binary	Whether or not this participant actively uses dopamine agonists	Yes (1) or No (0)
SYMBOLDIGIT	Continuous	Composed score of the Symbol and Digits task, indicating general cognitive capability	
MONTHSSINCEDIAG	Continuous	Number of months between the measurement and diagnosis	

Patient characteristics (depression)

*Supplementary Table 5 - **Patient characteristics (depression)** - We subdivided the PD population based on depression, by using a clinical cut-off score for the BDI-II. To compare groups, we used a 2x2 ANOVA (med * DEP-group). For gender and dopamine agonist use, we performed a chi-square test for both ICD vs non-ICD and ON vs OFF medication. *p < 0.05, **p <0.01, ***p <0.001 & n.s. = not significant.*

	ON		OFF					
NAME	PD-DEP+	PD-DEP-	PD-DEP+	PD-DEP-	HC	Effect MED	Effect DEP	Effect MED * DEP
NUMBER OF PARTICIPANTS	34	98	10	48	60	n.s.	n.s.	n.s.
AGE	59.18 (8.41)	60.33 (9.9)	61.3 (9.27)	60.98 (9.3)	60 (9.61)	n.s.	n.s.	n.s.
GENDER (F/M)	17/17	52/45	06/Apr	19/29	27/33	n.s.	n.s.	n.s.
DEPRESSION (BDI)	19.5 (5.46)	6.44 (3.64)	18.4 (3.81)	6.48 (3.27)	4.6 (3.51)	n.s.	***	n.s.
ICD (QUIPRS)	17.03 (14.9)	7.24 (9.43)	15.6 (14.74)	7.85 (8.23)	21.98 (10.13)	n.s.	***	n.s.
ANXIETY (STAI:TRAIT)	48.38 (8.73)	32.68 (7.18)	50.3 (6.33)	31.71 (6.21)	33.76 (6.77)	n.s.	***	n.s.
DISEASE SEVERITY (UPDRS:ON)	32.68 (10.79)	24.36 (10.81)	30 (10.39)	27.48 (14.31)		n.s.	*	n.s.
DISEASE SEVERITY (UPDRS:OFF)	39.38 (11.81)	28.94 (10.86)	37.5 (11.85)	33.48 (13.85)		n.s.	**	n.s.
LEDD	702.53 (426.76)	505.32 (281.04)	496.59 (294.02)	413.86 (260.37)		*	*	n.s.
DOPAMINE AGONIST USE (Y/N)	17/17	31/67	02/08	19/22		n.s.	n.s.	n.s.
BRIXTON	14.12 (6.61)	13.53 (6.48)	20.1 (6.81)	13.92 (5.3)		*	**	*
SEMENTIC FLUENCY	24.09 (5.9)	25.88 (5.3)	25.5 (5.32)	25.6 (6.81)		n.s.	n.s.	n.s.
SYMBOLS & DIGITS	32.94 (7.27)	38.42 (8.3)	36.9 (4.65)	38.15 (5.88)		n.s.	*	n.s.
MONTHS SINCE DIAGNOSIS	28.53 (16.81)	24.09 (16.01)	32.1 (16.56)	33.02 (16.14)		n.s.	n.s.	n.s.
RESTING TREMOR	1.65 (2.14)	1.01 (1.31)	1.5 (2.01)	1.33 (2.06)		n.s.	n.s.	n.s.

Supplementary Figures

Region of interest masks

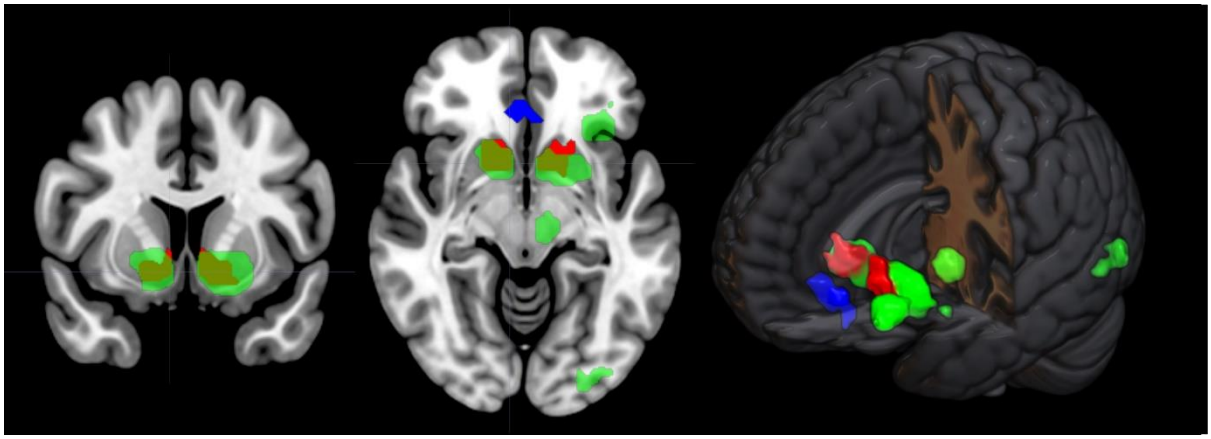

*Supplementary Figure 1 - **Masks used for region of interest analysis** - GREEN: reward prediction error response, consisting of the of the striatum, left insula, thalamus, V3 and V4. BLUE: expected value response, consisting of a part of the ventromedial prefrontal and orbitofrontal cortex. Masks are based on Chase et al..[1] RED: a secondary smaller RPE ROI (better matched to the size of the EV ROI), based on a mask of the ventral striatum, defined by Piray et al.,[2] based on a separate functional connectivity dataset, see supplementary figure 3.*

ROI analysis class-ICD vmPFC

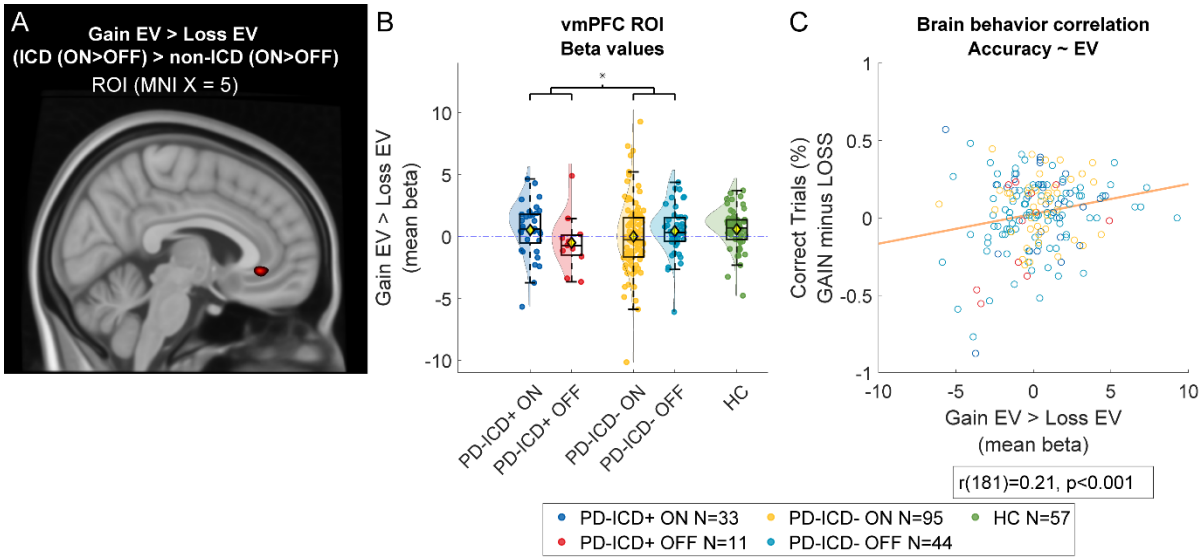

*Supplementary Figure 2 - **BOLD response for expected value per ICD group in the ventral medial PFC ROI – (A)** Medication induced a shift towards greater EV-related signal on GAIN vs LOSS trials in ICD patients vs non-ICD patients. Here the ROI (vmPFC) analysis is depicted. **(B)** Beta-values from the ROI in (A). **(C)** Brain behavior correlation; increased activity in the ROI vmPFC cluster correlated with increased accuracy during GAIN trials compared with LOSS trials across groups.*

ROI analysis class-ICD Ventral Striatum

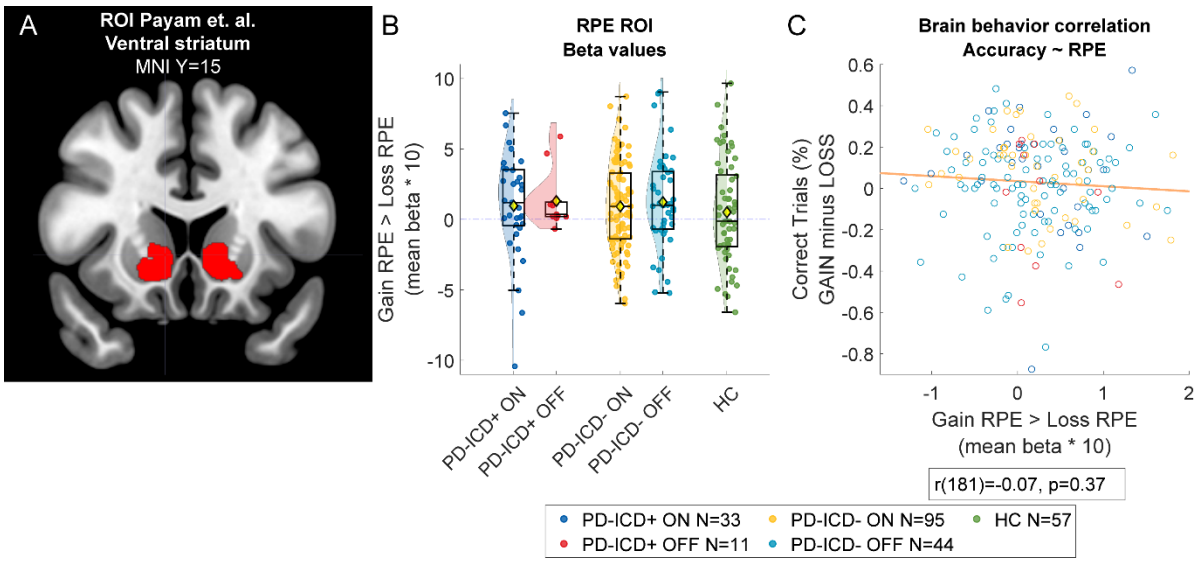

Supplementary Figure 3 – ***ROI BOLD response for reward prediction error per ICD group in the smaller RPE ROI of the ventral striatum as define by Piray et al.*** *–* ***(A)*** *The ROI comprised of both ventral striatal areas is depicted here.* ***(B)*** *Reward prediction error-related beta-values from the ROI (A).* ***(C)*** *Brain behavior correlation; increased activity in the VS ROI did not correlate with accuracy.*

Accuracy and WSLS behavior split by valence for ICD and Depression

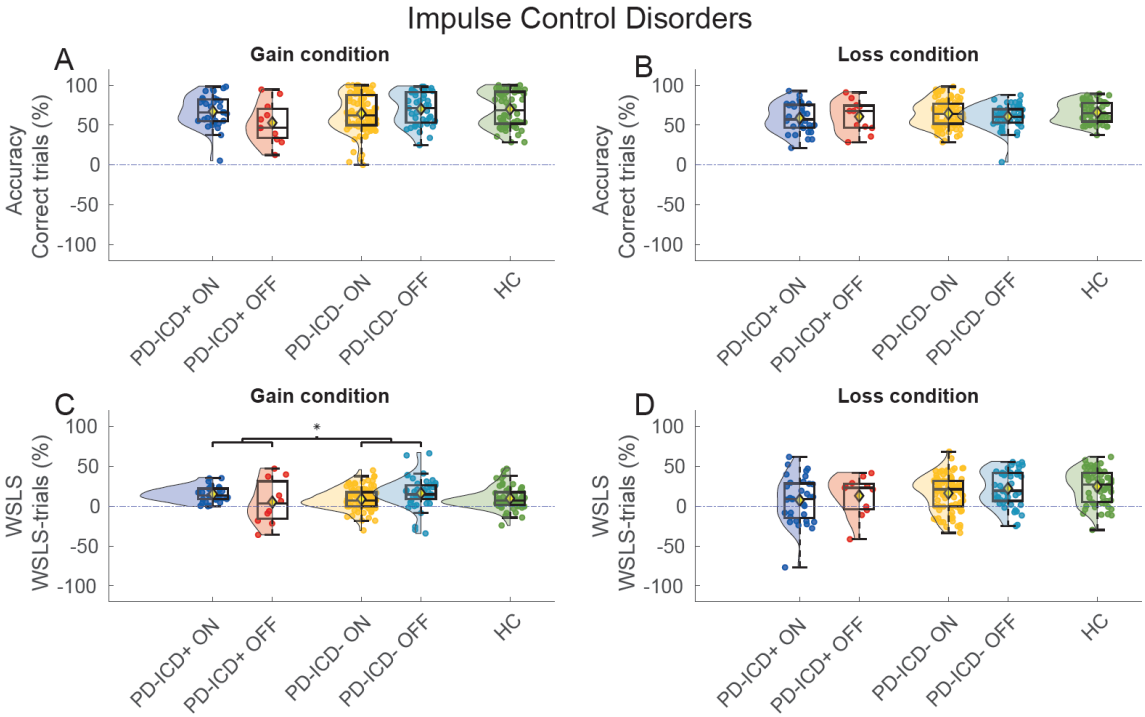

*Supplementary Figure 4 - **Accuracy and WSLS behavior split by valence for ICD** – – Here we split accuracy and WSLS performance for either **(A,C)** GAIN and **(B,D)** LOSS trials separately. Additionally **(A,B)** Show accuracy, while **(C,D)** show WSLS behavior. Only WSLS behavior during GAIN trials in ICD patients was a function of medication and ICD (p(stay) ~ Outcome * Group * ICD-class; GAIN trials only; brms 95% CI = [-0.27 -0.03])*

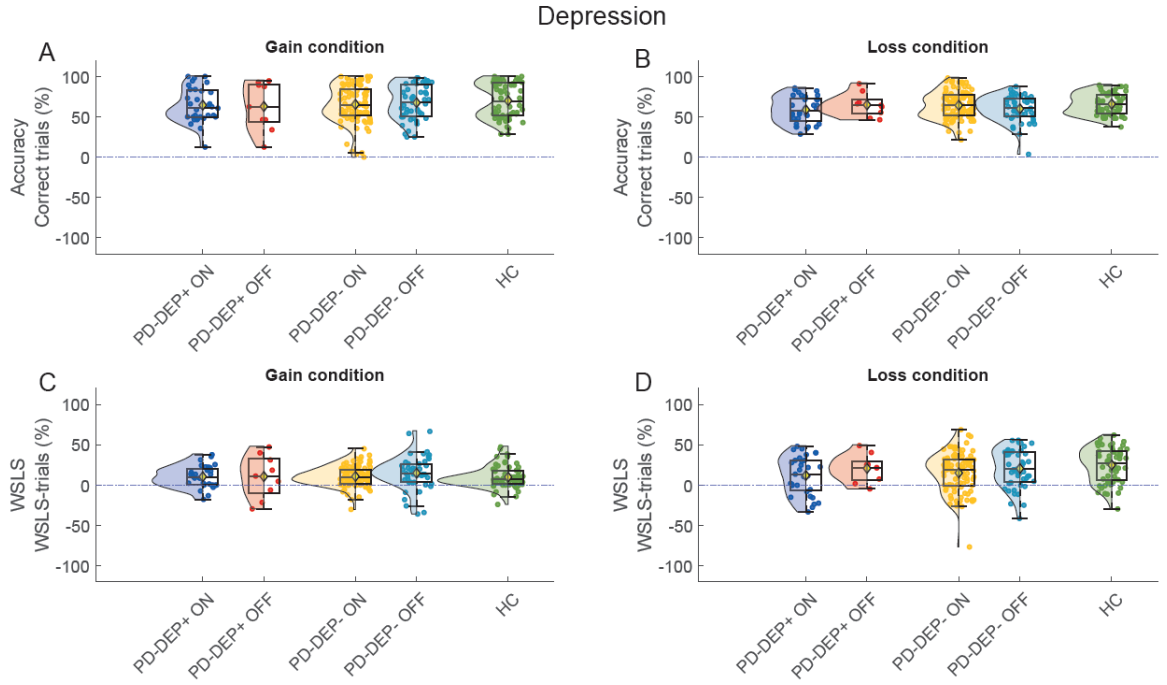

*Supplementary Figure 6 - **Accuracy and WSLS behavior split by valence for depression** – Here we split accuracy and WSLS performance for either **(A,C)** GAIN and **(B,D)** LOSS trials separately. Additionally **(A,B)** Show accuracy, while **(C,D)** show WSLS behavior.*

Subthreshold depiction of the effect of medication on EV-related signaling for GAIN vs LOSS in PD ICD patients

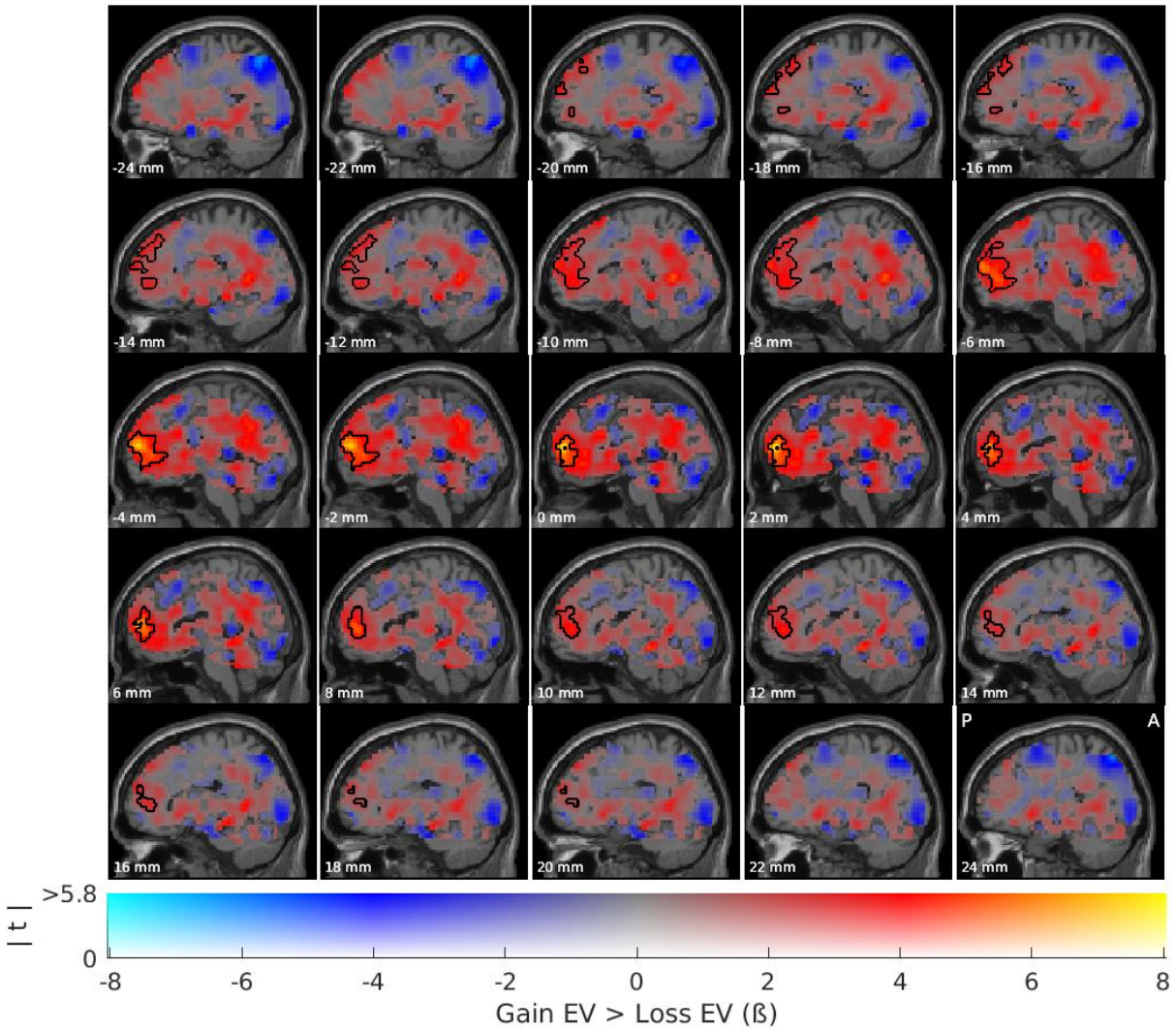

Supplementary Figure 5 - ***Subthreshold analysis of expected value related signaling in ICD patients (GAIN EV > LOSS EV)*** *- Red indicates increased EV signaling in GAIN trials compared to LOSS for ICD patients compared to non-ICD patients (i.e. ICD (ON > OFF) > non-ICD (ON > OFF)). The dual coded maps allow us to inspect sub-threshold activity, by simultaneously showing the contrast estimate β (color – contrast map) & significance, i.e. t-value (opacity - t-map). Thus, the color indicates the strength of the correlation, while the opacity indicates the significance. Clusters that survive multiple comparison correction (TFCE, FWE p<0.05) are encircled in black. The cluster in the medial prefrontal cluster showed increased activity in participants who also performed better in GAIN trials (compared to OFF trials), furthermore, beta values from this cluster correlated with accuracy (see main paper Fig. 6). Coordinates are in standard MNI space. Dual maps were implemented by Zandbelt[3] and introduced by Allen et al.,[4]*

Supplementary Methods

Participants

All PD patients were part of the Personalized Parkinson Project, which is a single-center, longitudinal observational study in 520 PD patients.[57] Patients are followed for a period of two years and are all tested at Radboud University Medical Center Nijmegen (Radboudumc). This study started in October 2017 and ran for five years until 2022. All patients were recruited through the Dutch national ParkinsonNet, the Dutch Parkinson Patient Association, Radboudumc, and social media.[57] Inclusion criteria were a diagnosis of idiopathic PD, a disease duration of <5 years, 18+ years of age and absence of contraindications for MRI. Furthermore patients had to be able (and willing) to give written informed consent.[57] Additionally we recruited 60 healthy controls, who were foremost spouses and caretakers of the PD patients.

Six patients were excluded, because they were unable to finish the RL task. Additionally, neuropsychiatric scores were incomplete for nine patients, who were excluded from the analyses in which those were required. Lastly, one patient was excluded specifically from the (f)MRI analyses due to low quality MRI data.

Clinical and neuropsychiatric questionnaire battery details

On day the second measurement day, on-site measurements started with an OFF-medication measurement on the MDS-Unified Parkinson's Disease Rating Scale (MDS-UPDRS), including Hoehn & Yahr scale. Next, patients took their standard medication dose, and were assessed ON medication with our clinical and neuropsychological test battery. This included the MDS-UPDRS, Hoehn & Yahr scale, 15 words test, Benton Judgement of Line Orientation, Brixton Executive Functioning test, Numbers and Letters pronunciation test,

Montreal Cognitive Assessment (MOCA), Semantic fluency & the Symbol Digit modalities test (SDMT), in addition to demographic and medical information (see Bloem *et al.*,[5] for a detailed description of these background neuropsychological tests). Furthermore, participants were asked to complete a set of neuropsychiatric questionnaires at home including the Beck Depression Inventory II (BDI), the Questionnaire for Impulsive-Compulsive Disorders in Parkinson's Disease-Rating Scale (QUIP-rs) and the State Trait Anxiety Inventory for Adults (STAI).

Neuropsychiatric subgroups

Analyses were stratified by the presence of clinical depression and ICDs. Depressive symptoms were quantified with the Beck Depression Inventory II (BDI). Patients with a BDI score >= 14 were marked as the PD-DEP+ subtype, according to Beck *et al.*.[6] Impulse control disorder was assessed with the Questionnaire for Impulsive-Compulsive Disorders in Parkinson's disease Rating Scale (QUIP-rs). Following Evans *et al.*[7] we classified a patient as PD-ICD+ if any of the individual QUIP-rs sub scores reached the cutoff value: for pathological gambling >= 6, compulsive buying >= 8, hypersexuality >= 8, binge eating >=7, combined ICDs (without hobbyism and punding) >= 10 or hobbyism and punding >= 7. For an overview for the number of patients with each disorder, see Supplementary Table 1.

MRI analysis

Image acquisition

All scanning was performed at the Donders Centre for Cognitive Neuroimaging, which is part of the Donders Institute for Brain, Cognition and Behaviour (Nijmegen, the Netherlands). All images were acquired with a 3T MAGNETOM Prisma MR scanner (Siemens AG, Healthcare Sector, Erlangen, Germany) in combination with a 32-channel head coil. T1 weighted

anatomical images were acquired with the MPRAGE sequence (Magnetization-prepared rapid gradient-echo). The scanner settings were set to; TR=2300ms, TE=3ms, TI=1100ms, flip-angle=0.8°, voxel-size= 1.0x1.0x1.0mm, number of slices = 192, FOV = 256mm, scanning-time = 321s. BOLD images were acquired with a multi-echo sequence. The scanner settings were set to; TR=2240ms, TE1=10.00ms, TE2=19.9ms, TE3=29.8ms, TE4=39.7ms, TE5=49.6ms, flip-angle=90°, voxel-size= 3.5x3.5x3.0mm, number of slices = 32, distance-factor=17%, FOV = 224mm.

Image preprocessing

First we used the PAID algorithm (implemented by the BIDSCOINER toolbox[61]) to manually combine the individual fMRI echoes into one image. Preprocessing on this scan was performed with fMRIPrep 20.2.1.[62] In short, the anatomical images were adjusted for non-uniformity, skill stripped and segmented into white matter, grey matter and cerebral spinal fluid. Volume based spatial normalization was applied to transform the images into MNI space. The BOLD images were skull-stripped, co-registered to the T1 reference image with six degrees of freedom and corrected for slice-timing in one transformation. This pre-processed BOLD image was transformed from native to MNI space and smoothed with an 8mm kernel. For a detailed description of the processing pipeline & sequence details see supplementary methods.

Regions of interest analysis

To investigate group differences in relevant BOLD responses, we focused our analyses on those regions known to encode RPE and EV respectively. Specifically, we selected two regions (or networks) of interests (ROI) based on an existing meta-analysis of prior fMRI studies of RL.[1] We downloaded the ROI files from the ANIMA database that stores the relevant meta-analysis.[8] The RPE ROI comprised the striatum, left insula, thalamus, V3 and

V4. The EV ROI consisted of one cluster compromising a part of the ventromedial prefrontal and orbitofrontal cortex. In supplementary analyses, we controlled for the differences in size between these RPE and EV ROIs by focusing the RPE analyses on a smaller functionally defined ROI, comprising only the ventral striatum, as identified based on an independent functional connectivity analyses by Piray et al.[2] All masks were applied during the TFCE analysis. All ROIs were chosen a priori, for a visual representation of the ROIs see supplementary Fig. 1.

Fmriprep preprocessing

Results included in this manuscript come from preprocessing performed using fMRIPrep 20.2.1[9,10] (RRID:SCR_016216), which is based on Nipype 1.5.1[11,12] (RRID:SCR_002502).

Anatomical data preprocessing

A total of 1 T1-weighted (T1w) images were found within the input BIDS dataset.The T1-weighted (T1w) image was corrected for intensity non-uniformity (INU) with N4BiasFieldCorrection[13], distributed with ANTs 2.3.3[14] (RRID:SCR_004757), and used as T1w-reference throughout the workflow. The T1w-reference was then skull-stripped with a Nipype implementation of the antsBrainExtraction.sh workflow (from ANTs), using OASIS30ANTs as target template. Brain tissue segmentation of cerebrospinal fluid (CSF), white-matter (WM) and gray-matter (GM) was performed on the brain-extracted T1w using fast (FSL 5.0.9[15], RRID:SCR_002823). Brain surfaces were reconstructed using recon-all (FreeSurfer 6.0.1[16], RRID:SCR_001847), and the brain mask estimated previously was refined with a custom variation of the method to reconcile ANTs-derived and FreeSurfer-derived segmentations of the cortical gray-matter of Mindboggle[17] (RRID:SCR_002438). Volume-based spatial normalization to two standard spaces (MNI152NLin6Asym, MNI152NLin2009cAsym) was performed through nonlinear registration with

antsRegistration (ANTs 2.3.3), using brain-extracted versions of both T1w reference and the T1w template. The following templates were selected for spatial normalization: FSL's MNI ICBM 152 non-linear 6th Generation Asymmetric Average Brain Stereotaxic Registration Model[18] [RRID:SCR_002823; TemplateFlow ID: MNI152NLin6Asym], ICBM 152 Nonlinear Asymmetrical template version 2009c[19] [RRID:SCR_008796; TemplateFlow ID: MNI152NLin2009cAsym],

Functional data preprocessing

For each of the 2 BOLD runs found per subject (across all tasks and sessions), the following preprocessing was performed. First, a reference volume and its skull-stripped version were generated by aligning and averaging 1 single-band references (SBRefs). Susceptibility distortion correction (SDC) was omitted. The BOLD reference was then co-registered to the T1w reference using bbregister (FreeSurfer) which implements boundary-based registration.[20] Co-registration was configured with six degrees of freedom. Head-motion parameters with respect to the BOLD reference (transformation matrices, and six corresponding rotation and translation parameters) are estimated before any spatiotemporal filtering using mcflirt (FSL 5.0.9[21]). BOLD runs were slice-time corrected using 3dTshift from AFNI 20160207[22] (RRID:SCR_005927). First, a reference volume and its skull-stripped version were generated using a custom methodology of fMRIPrep. The BOLD time-series (including slice-timing correction when applied) were resampled onto their original, native space by applying the transforms to correct for head-motion. These resampled BOLD time-series will be referred to as preprocessed BOLD in original space, or just preprocessed BOLD. The BOLD time-series were resampled into standard space, generating a preprocessed BOLD run in MNI152NLin6Asym space. First, a reference volume and its skull-stripped version were generated using a custom methodology of fMRIPrep. Automatic removal of motion artifacts using independent component analysis (ICA-AROMA[23]) was

performed on the preprocessed BOLD on MNI space time-series after removal of non-steady state volumes and spatial smoothing with an isotropic, Gaussian kernel of 6mm FWHM (full-width half-maximum). Corresponding "non-aggresively" denoised runs were produced after such smoothing. Additionally, the "aggressive" noise-regressors were collected and placed in the corresponding confounds file. Several confounding time-series were calculated based on the preprocessed BOLD: framewise displacement (FD), DVARS and three region-wise global signals. FD was computed using two formulations following Power[24] (absolute sum of relative motions) and Jenkinson[21] (relative root mean square displacement between affines). FD and DVARS are calculated for each functional run, both using their implementations in Nipype (following the definitions by Power *et al.*[24]). The three global signals are extracted within the CSF, the WM, and the whole-brain masks. Additionally, a set of physiological regressors were extracted to allow for component-based noise correction (CompCor[25]). Principal components are estimated after high-pass filtering the preprocessed BOLD time-series (using a discrete cosine filter with 128s cut-off) for the two CompCor variants: temporal (tCompCor) and anatomical (aCompCor). tCompCor components are then calculated from the top 2% variable voxels within the brain mask. For aCompCor, three probabilistic masks (CSF, WM and combined CSF+WM) are generated in anatomical space. The implementation differs from that of Behzadi *et al.*[25] in that instead of eroding the masks by 2 pixels on BOLD space, the aCompCor masks are subtracted a mask of pixels that likely contain a volume fraction of GM. This mask is obtained by dilating a GM mask extracted from the FreeSurfer's aseg segmentation, and it ensures components are not extracted from voxels containing a minimal fraction of GM. Finally, these masks are resampled into BOLD space and binarized by thresholding at 0.99 (as in the original implementation). Components are also calculated separately within the WM and CSF masks. For each CompCor decomposition, the k components with the largest singular values are retained, such that the

retained components' time series are sufficient to explain 50 percent of variance across the nuisance mask (CSF, WM, combined, or temporal). The remaining components are dropped from consideration. The head-motion estimates calculated in the correction step were also placed within the corresponding confounds file. The confound time series derived from head motion estimates and global signals were expanded with the inclusion of temporal derivatives and quadratic terms for each[26]. Frames that exceeded a threshold of 0.5 mm FD or 1.5 standardised DVARS were annotated as motion outliers. All resamplings can be performed with a single interpolation step by composing all the pertinent transformations (i.e. head-motion transform matrices, susceptibility distortion correction when available, and co-registrations to anatomical and output spaces). Gridded (volumetric) resamplings were performed using antsApplyTransforms (ANTs), configured with Lanczos interpolation to minimize the smoothing effects of other kernels[27]. Non-gridded (surface) resamplings were performed using mri_vol2surf (FreeSurfer).

Many internal operations of fMRIPrep use Nilearn 0.6.2[28] (RRID:SCR_001362), mostly within the functional processing workflow. For more details of the pipeline, see the section corresponding to workflows in fMRIPrep's documentation.

Instruction for the participant

Prior to the training block, the following instructions were given to the participant. The instructions were adjusted from Schmidt et al., [29] and were translated to Dutch. After the training session, participants could ask questions to the assessor.

DUTCH (instructions as they were given to the participant)

"In de scanner zult u een tweede taak uitvoeren, die ook 10 minuten zal duren. U gaat nu een korte versie van deze taak uitvoeren. Hier kunt u de instructies lezen. Net als eerder, gebruikt

u hier weer de pijltoetsen om verder- of terug te gaan. Vraag het gerust aan de onderzoekers als er iets onduidelijk is, en laat het ze weten als u aan het eind van deze instructies bent gekomen."

"Twee symbolen verschijnen links en rechts van het kruis in het midden van het scherm. Kies één van de twee symbolen via het toetsenbord. Het rechter symbool kiest u door 1 in te toetsen, voor het linker symbool toetst u 2."

"Er verschijnt een pijl onder het symbool dat u gekozen heeft."

"Nadat u een symbool gekozen heeft, kunt u: niks krijgen, tien euro winnen of tien euro verliezen."

"Om de kans te hebben om te winnen, moet u een keuze maken en één van de twee knoppen indrukken. Als u niets doet of te langzaam reageert, zult u het volgende zien."

"De twee symbolen die op hetzelfde scherm worden weergegeven, zijn niet equivalent in termen van uitkomst: bij de ene heb je meer kans om niets te krijgen dan bij de ander. Elk symbool heeft zijn eigen betekenis, ongeacht waar (links of rechts van het centrale kruis) of wanneer deze wordt weergegeven."

"Het doel van het spel is om zo veel mogelijk geld te winnen."

"Veel succes! ."

"Dit is het einde van de instructies. Neem nu nog even contact op met de onderzoeker en geef aan of u de taak goed begrijpt, of dat extra uitleg nodig is. De onderzoeker zal nu de toetsen die u voor de taak gaat gebruiken aanwijzen. De taak begint pas als u één van de antwoordtoetsen indrukt."

ENGLISH (translated from the text above)

“In the scanner you will perform a second task, which will also take 10 minutes. You will now perform a short version of this task. Here you can read the instructions. Just as before, you will use the arrow keys to continue or go back. Please ask the assessor if anything is unclear and let them know when you have finished these instructions.

“Two symbols will appear left and right of the cross in the centre of the screen. Choose one of the two symbols with the keyboard. You will choose the right symbol by pressing 1, for the left symbol you press 2.”

“An arrow will appear under the symbol you have chosen.”

“After you have chosen a symbol, you can either receive nothing, win 10 euros or lose 10 euros.”

“To be able to win, make a choice by pressing one of the two buttons. If you do not press in time you will see the following.”

“The two symbols displayed on the screen, are not equivalent in terms of outcome. One will give a higher chance on not receiving anything than the other. Every symbol has its own meaning, independent of the place (left or right of the cross), or when it is displayed.”

“The goal of the game is to make as much money as possible”

“Goodluck!”

“This is the end of the instructions. Please contact the assessor and tell them whether you fully understand the task or whether additional help is needed. The assessor will point you to the buttons used in the task. The task will start when you press one of the answer buttons.”

Supplementary Results

Simple effects analyses and breakdown of higher order interaction effects

Medication increased WSLS on GAIN more than LOSS trials, in PD ON compared with healthy controls (p(stay) ~ medication * valence * previous outcome)

This three-way interaction was driven by LOSSES (previous outcome * group; brms 95% CI = [-0.19 -0.02]), but not GAINS (previous outcome * group; brms 95% CI = [-0.08 0.10]), by patients ON medication (valence * previous outcome; brms 95% CI = [0.02 0.14]), but not HC (valence * previous outcome; brms 95% CI = [-0.10 0.09]) and by PUNISHMENTS on the previous outcome (valence * group; brms 95% CI = [-0.17 -0.002]), but not WINS (valence * group; brms 95% CI = [-0.08 0.12]). Further simple effects analyses revealed that this effect was due to patients ON medication *shifting* less often than HC after LOSSES (i.e. -€10)(main effect of medication; brms 95% CI = [0.05 0.22]). Thus, compared with HC, PD patients ON medication were less sensitive to punishment, although this did not surface in an ON vs HC difference in choice accuracy (valence * group; brms 95% CI = [-0.18 0.04], main effect of group; brms 95% CI = [-0.26 0.02])(see Fig 1C).

Medication increased accuracy on GAIN vs LOSS trials in PD with ICD (p($cue_{correct}$) ~ ICD-class * medication * valence)

The simple two-way ICD-class * medication effects on accuracy for GAIN and LOSS trials separately were not significant, so the effect on accuracy is best described as a change in the balance between learning from GAINS versus LOSSES.

Medication increased WSLS tendency on GAIN vs LOSS trials in patients with ICD (p(stay) ~ ICD-class * medication * valence * previous outcome)

Breaking down the interaction for the probability of staying into its simple interaction effects revealed that the WSLS effect was driven by behavior during REWARDED (i.e. WIN) trials (valence * ICD-class * medication; brms 95% CI = [-0.28 -0.04]), but not PUNISHED (i.e. LOSS) trials (valence * ICD-class * medication; brms 95% CI = [-0.08 0.12]), by the GAIN condition (ICD-class * medication * previous outcome; brms 95% CI = [-0.26 -0.02]) but not LOSS condition (ICD-class * medication * previous outcome; brms 95% CI = [-0.08 0.15]), by patients ON medication (valence * ICD-class * previous outcome; brms 95% CI = [0.06 0.18]) but not patients OFF medication, and by patients with ICD (valence * previous outcome * medication; brms 95% CI =[-0.27 -0.02]) but not patients without ICD. Thus, sensitivity to REWARDS/GAINS is enhanced in patients ON versus OFF medication, but only when they have ICD.

Reaction time analyses

The effects on accuracy were accompanied by similar effects on reaction times, which also varied as a function of valence, medication, and neuropsychiatric vulnerability (valence * medication * class-ICD; brms 95% CI = [0.001 0.033]). Thus, there was a medication * valence interaction in patients with ICD (valence * medication; brms 95% CI = [0.001 0.060]), but not in patients without ICDs (valence * medication; brms 95% CI = [-0.01 0.01]). This means that ICD patients ON medication responded faster during GAIN vs LOSS trials than patients OFF medication (Fig. 3G). This shows that ICD patients ON medication are not only more accurate, but also faster during GAIN trials. Across all participants, subjects were slower for LOSS trials compared with GAIN trials (main effect of valence; brms 95% CI = [-0.13 -0.10]), but there was no interaction with medication (valence *

medication; brms 95% CI = [-0.01 0.01]), and no main effect of medication (brms 95% CI = [-0.05 0.01]). However, the effect of reaction time was no longer significant after including the use of dopamine agonists (valence * group * ICD-class; agonist use as confound; brms 95% CI = [-0.031 0.001]).

The finding that medication-related increases in accuracy on gain versus loss trials are accompanied by medication-related increases in RTs on gain versus loss trials supports the hypothesis that medication boosts the efficiency of evidence accumulation for value-based choice, a mechanism that has previously been shown to implicate the vmPFC.[30] The parallel effects on accuracy and RT also indicate that the effect is unlikely to reflect a strategic change of a decision threshold, due to biased speed-accuracy trade-off, or of a decision starting point, due to changes in prior beliefs about which action is valuable. Future computational modeling of both RT distributions and choice sequences simultaneously using an RL-drift diffusion model[31,32] is required to establish this hypothesis more firmly.

Supplementary Discussion

Differences between Voon et al. and this work

The most striking difference between the Voon et al. study and the current study is the double amount of practice trials (180 in the Voon study vs 56 in the current study). Moreover, the PD ICD patients in the Voon study had a longer cue evaluation time (cue presented for 4.5s + 1s RT) compared with those in the current study (cue presentation + RT = 2.5s). In addition, PD patients with ICD in the Voon et al study showed increased error rate on a spatial WM task compared with the non-ICD patients. Based on these observations, we argue that patients in the Voon et al study might have been less likely to rely on a WM strategy, and more likely to rely on an RPE-based RL strategy to solve the task.

Confounding effects

Patients with ICDs had a higher daily dose of dopaminergic medication and used dopamine agonists more often than did patients without ICDs. This raises the question whether the medication-related increase in gain versus loss-based choice is due selectively to the presence of ICDs or rather reflects the fact that these ICD patients took higher drug doses and/or dopamine receptor agonists. However, the interaction between ICD and medication on both accuracy and WSLS (albeit not response speed) remained significant, even after correcting for dopamine medication dose or agonist use, suggesting that this is not the case. By analogy, the observation that PD-ICD patients performed more poorly than PD patients without ICDs on the Symbol Digit modalities test, i.e., exhibited lower mental processing speed, an effect often associated with general intelligence[33], raises the question whether the disproportionate medication effect reflects variability in intelligence rather than the presence of comorbid ICDs. Again, however, our interactive effects of ICDs and medication on accuracy, reaction

time and WSLS behavior survived correction for the digit-symbol score, suggesting this was not the case. Furthermore, our interactive effects of ICD and medication also remained significant after correcting for gender (more men with PD ICD than women[34]), for depression and anxiety scores (higher in PD ICD than PD non-ICD[35]). A final confounding factor is the time difference between the OFF and ON state MRI session. The OFF state measurement was always after the ON state measurement.

Depression does not affect accuracy, RT or WSLS behavior

In the current work, there was no evidence for a role for depression (BDI-II > 14) in the medication effects on reaction times, accuracy or win-stay-lose-shift behavior. This is surprising, because prior work has demonstrated disproportionate vulnerability to medication-related decreases in sensitivity to losses in PD patients with depression compared with PD patients without depression: such disproportionate dopamine-related decreases in loss sensitivity in PD with depression versus PD without depression has been shown in the context of both risky choice[36] as well as reversal learning[37] and, like the effects in PD ICDs, were argued to reflect deficient autoregulatory mechanisms in the ventral striatum, including decreased striatal DAT[38-41] and decreased D2/D3 receptor availability[42]. The lack of an effect of depression in the current study is particularly puzzling given the large literature on RL and value-based decision making deficits in patients with major depression without PD[43-49] (but see Brolsma et al.,[50]). Indeed, it raises the question whether depressive symptoms in our patient group were sufficiently severe to detect any such effect. An alternative possibility is that the task was not optimized to detect depression-dependent incremental RL deficits, since the absence of striatal RPE signaling abnormalities might be accounted for by increased opportunity for reliance on WM (see discussion). Finally, it remains possible that the sample

size of the PD depressed group OFF medication (n=10) was not large enough to detect a reliable effect.

A twelve hour wash out period for dopaminergic drugs, might not be sufficient

The absence of abnormal striatal RPE signaling might be explained by insufficient washout of dopaminergic medication. Patients withdrew from their dopaminergic medication overnight for at least 12 hours prior to their assessments. It has been shown that overnight withdrawal is less effective in reducing dopamine levels than is the natural OFF state.[51] While we cannot exclude the possibility that striatal RPE deficits would have been revealed with more effective medication withdrawal, the presents results do demonstrate that frontal EV signals at choice are more sensitive to manipulation of dopamine than are striatal RPE signals at outcome.

References

1. Chase HW, Kumar P, Eickhoff SB, Dombrovski AY. Reinforcement learning models and their neural correlates: An activation likelihood estimation meta-analysis. *Cognitive, affective & behavioral neuroscience.* 2015;15(2):435-459.
2. Piray P, den Ouden HEM, van der Schaaf ME, Toni I, Cools R. Dopaminergic Modulation of the Functional Ventrodorsal Architecture of the Human Striatum. *Cerebral Cortex.* 2015;27(1):485-495.
3. *Slice display* [computer program]. figshare; 2017.
4. Allen EA, Erhardt EB, Calhoun VD. Data visualization in the neurosciences: overcoming the curse of dimensionality. *Neuron.* 2012;74(4):603-608.
5. Bloem BR, Marks WJ, Silva de Lima AL, et al. The Personalized Parkinson Project: examining disease progression through broad biomarkers in early Parkinson's disease. *BMC Neurology.* 2019;19(1):160.
6. Beck AT, Steer RA, Brown GK. *Beck depression inventory (BDI-II).* Vol 10: Pearson London, UK; 1996.
7. Evans AH, Okai D, Weintraub D, et al. Scales to assess impulsive and compulsive behaviors in Parkinson's disease: Critique and recommendations. *Movement disorders : official journal of the Movement Disorder Society.* 2019;34(6):791-798.
8. al. Ce. Reinforcement learning models and their neural correlates: An activation likelihood estimation meta-analysis. 2022; https://anima.fz-juelich.de/studies/Chase_ReinforcementLearningALE_2015. Accessed 15-07-2022, 2022.
9. Esteban O, Markiewicz CJ, Blair RW, et al. fMRIPrep: a robust preprocessing pipeline for functional MRI. *Nature Methods.* 2019;16(1):111-116.
10. *fMRIPrep: a robust preprocessing pipeline for functional MRI* [computer program]. Version 22.0.2: Zenodo; 2022.
11. *nipy/nipype: 1.8.3* [computer program]. Version 1.8.3: Zenodo; 2022.
12. Gorgolewski K, Burns C, Madison C, et al. Nipype: A Flexible, Lightweight and Extensible Neuroimaging Data Processing Framework in Python. 2011;5.
13. Tustison NJ, Avants BB, Cook PA, et al. N4ITK: Improved N3 Bias Correction. *IEEE Transactions on Medical Imaging.* 2010;29(6):1310-1320.
14. Avants BB, Epstein CL, Grossman M, Gee JC. Symmetric diffeomorphic image registration with cross-correlation: Evaluating automated labeling of elderly and neurodegenerative brain. *Medical Image Analysis.* 2008;12(1):26-41.
15. Zhang Y, Brady M, Smith S. Segmentation of brain MR images through a hidden Markov random field model and the expectation-maximization algorithm. *IEEE Transactions on Medical Imaging.* 2001;20(1):45-57.
16. Dale AM, Fischl B, Sereno MI. Cortical Surface-Based Analysis: I. Segmentation and Surface Reconstruction. *NeuroImage.* 1999;9(2):179-194.
17. Klein A, Ghosh SS, Bao FS, et al. Mindboggling morphometry of human brains. *PLoS computational biology.* 2017;13(2):e1005350.
18. Evans AC, Janke AL, Collins DL, Baillet S. Brain templates and atlases. *NeuroImage.* 2012;62(2):911-922.
19. Fonov VS, Evans AC, McKinstry RC, Almli CR, Collins DL. Unbiased nonlinear average age-appropriate brain templates from birth to adulthood. *NeuroImage.* 2009;47:S102.
20. Greve DN, Fischl B. Accurate and robust brain image alignment using boundary-based registration. *NeuroImage.* 2009;48(1):63-72.

21. Jenkinson M, Bannister P, Brady M, Smith S. Improved Optimization for the Robust and Accurate Linear Registration and Motion Correction of Brain Images. *NeuroImage.* 2002;17(2):825-841.
22. Cox RW, Hyde JS. Software tools for analysis and visualization of fMRI data. 1997;10(4-5):171-178.
23. Pruim RHR, Mennes M, van Rooij D, Llera A, Buitelaar JK, Beckmann CF. ICA-AROMA: A robust ICA-based strategy for removing motion artifacts from fMRI data. *NeuroImage.* 2015;112:267-277.
24. Power JD, Mitra A, Laumann TO, Snyder AZ, Schlaggar BL, Petersen SE. Methods to detect, characterize, and remove motion artifact in resting state fMRI. *NeuroImage.* 2014;84:320-341.
25. Behzadi Y, Restom K, Liau J, Liu TT. A component based noise correction method (CompCor) for BOLD and perfusion based fMRI. *NeuroImage.* 2007;37(1):90-101.
26. Satterthwaite TD, Elliott MA, Gerraty RT, et al. An improved framework for confound regression and filtering for control of motion artifact in the preprocessing of resting-state functional connectivity data. *NeuroImage.* 2013;64:240-256.
27. Lanczos C. Evaluation of Noisy Data. 1964;1(1):76-85.
28. Abraham A, Pedregosa F, Eickenberg M, et al. Machine learning for neuroimaging with scikit-learn. 2014;8.
29. Schmidt L, Braun EK, Wager TD, Shohamy D. Mind matters: placebo enhances reward learning in Parkinson's disease. *Nature neuroscience.* 2014;17(12):1793-1797.
30. Lim S-L, O'Doherty JP, Rangel A. The Decision Value Computations in the vmPFC and Striatum Use a Relative Value Code That is Guided by Visual Attention. 2011;31(37):13214-13223.
31. Fontanesi L, Gluth S, Spektor MS, Rieskamp J. A reinforcement learning diffusion decision model for value-based decisions. *Psychonomic Bulletin & Review.* 2019;26(4):1099-1121.
32. Pedersen ML, Frank MJ. Simultaneous Hierarchical Bayesian Parameter Estimation for Reinforcement Learning and Drift Diffusion Models: a Tutorial and Links to Neural Data. *Computational brain & behavior.* 2020;3(4):458-471.
33. Jaeger J. Digit Symbol Substitution Test: The Case for Sensitivity Over Specificity in Neuropsychological Testing. *Journal of clinical psychopharmacology.* 2018;38(5):513-519.
34. Joutsa J, Martikainen K, Vahlberg T, Kaasinen V. Effects of dopamine agonist dose and gender on the prognosis of impulse control disorders in Parkinson's disease. *Parkinsonism & Related Disorders.* 2012;18(10):1079-1083.
35. Marín-Lahoz J, Sampedro F, Martinez-Horta S, Pagonabarraga J, Kulisevsky J. Depression as a Risk Factor for Impulse Control Disorders in Parkinson Disease. *Annals of neurology.* 2019;86(5):762-769.
36. Timmer MHM, Sescousse G, Esselink RAJ, Piray P, Cools R. Mechanisms Underlying Dopamine-Induced Risky Choice in Parkinson's Disease With and Without Depression (History). *Computational psychiatry (Cambridge, Mass).* 2018;2:11-27.
37. Cools R, Tichelaar JG, Helmich RCG, et al. Role of dopamine and clinical heterogeneity in cognitive dysfunction in Parkinson's disease. *Progress in brain research.* 2022;269(1):309-343.
38. Remy P, Doder M, Lees A, Turjanski N, Brooks D. Depression in Parkinson's disease: loss of dopamine and noradrenaline innervation in the limbic system. *Brain.* 2005;128(Pt 6):1314-1322.

39. Vriend C, Raijmakers P, Veltman DJ, et al. Depressive symptoms in Parkinson's disease are related to reduced [123I]FP-CIT binding in the caudate nucleus. *Journal of neurology, neurosurgery, and psychiatry.* 2014;85(2):159-164.
40. Weintraub D, Newberg AB, Cary MS, et al. Striatal dopamine transporter imaging correlates with anxiety and depression symptoms in Parkinson's disease. *Journal of nuclear medicine : official publication, Society of Nuclear Medicine.* 2005;46(2):227-232.
41. Rektorova I, Srovnalova H, Kubikova R, Prasek J. Striatal dopamine transporter imaging correlates with depressive symptoms and tower of London task performance in Parkinson's disease. *Movement disorders : official journal of the Movement Disorder Society.* 2008;23(11):1580-1587.
42. Boileau I, Guttman M, Rusjan P, et al. Decreased binding of the D3 dopamine receptor-preferring ligand [11C]-(+)-PHNO in drug-naive Parkinson's disease. *Brain.* 2009;132(Pt 5):1366-1375.
43. Kunisato Y, Okamoto Y, Ueda K, et al. Effects of depression on reward-based decision making and variability of action in probabilistic learning. *Journal of Behavior Therapy and Experimental Psychiatry.* 2012;43(4):1088-1094.
44. Reinen JM, Whitton AE, Pizzagalli DA, et al. Differential reinforcement learning responses to positive and negative information in unmedicated individuals with depression. *European Neuropsychopharmacology.* 2021;53:89-100.
45. Admon R, Pizzagalli DA. Dysfunctional reward processing in depression. *Current Opinion in Psychology.* 2015;4:114-118.
46. Eshel N, Roiser JP. Reward and punishment processing in depression. *Biological psychiatry.* 2010;68(2):118-124.
47. Huys QJM. *Reinforcers and control: Towards a computational aetiology of depression* [Ph.D.]. Ann Arbor, University of London, University College London (United Kingdom); 2007.
48. Diego A. Pizzagalli PD, Avram J. Holmes AM, Daniel G. Dillon PD, et al. Reduced Caudate and Nucleus Accumbens Response to Rewards in Unmedicated Individuals With Major Depressive Disorder. 2009;166(6):702-710.
49. Robinson OJ, Cools R, Carlisi CO, Sahakian BJ, Drevets WC. Ventral Striatum Response During Reward and Punishment Reversal Learning in Unmedicated Major Depressive Disorder. *American Journal of Psychiatry.* 2012;169(2):152-159.
50. Brolsma SCA, Vrijsen JN, Vassena E, et al. Challenging the negative learning bias hypothesis of depression: reversal learning in a naturalistic psychiatric sample. *Psychological medicine.* 2022;52(2):303-313.
51. Cilia R, Cereda E, Akpalu A, et al. Natural history of motor symptoms in Parkinson’s disease and the long-duration response to levodopa. *Brain.* 2020;143(8):2490-2501.